International Journal of Biological Macromolecules 141 (2019) 855–867

Contents lists available at ScienceDirect

International Journal of Biological Macromolecules

journal homepage: www.elsevier.com/locate/ijbiomac

Structural and biochemical insights into an engineered high-redox potential laccase overproduced in *Aspergillus*

Felipe de Salas [a], Rubén Cañadas [b], Gerard Santiago [b], Alicia Virseda-Jerez [c], Jesper Vind [d], Patrizia Gentili [e], Angel T. Martínez [a], Víctor Guallar [b,f], Inés G. Muñoz [c], Susana Camarero [a,*]

[a] Centro de Investigaciones Biológicas, CSIC. Ramiro de Maeztu 9, 28040 Madrid, Spain
[b] Barcelona Supercomputing Center, Jordi Girona 29, 08034 Barcelona, Spain
[c] Crystallography and Protein Engineering Unit, Structural Biology Programme, CNIO, Melchor Fernández Almagro 3, 28029 Madrid, Spain
[d] Novozymes, A/S Krogshoejvej 36, 2880 Bagsvaerd, Denmark
[e] Dipartimento di Chimica and IMC-CNR Sezione Meccanismi di Reazione, Università degli Studi La Sapienza, P. le A. Moro 5, I-00185 Roma, Italy
[f] ICREA: Institució Catalana de Recerca i Estudis Avancats, Passeig Lluís Companys 23, 08010 Barcelona, Spain

ARTICLE INFO

Article history:
Received 11 July 2019
Received in revised form 27 August 2019
Accepted 6 September 2019
Available online 07 September 2019

Keywords:
Fungal laccase
Aspergillus oryzae
Crystal structure
SAXS
Kinetics
Circular dichroism

ABSTRACT

Fungal laccases have great potential as biocatalysts oxidizing a variety of aromatic compounds using oxygen as co-substrate. Here, the crystal structure of 7D5 laccase (PDB 6H5Y), developed in *Saccharomyces cerevisiae* and overproduced in *Aspergillus oryzae*, is compared with that of the wild type produced by basidiomycete PM1 (*Coriolopsis* sp.), PDB 5ANH. SAXS showed both enzymes form monomers in solution, 7D5 laccase with a more oblate geometric structure due to heavier and more heterogeneous glycosylation. The enzyme presents superior catalytic constants towards all tested substrates, with no significant change in optimal pH or redox potential. It shows noticeable high catalytic efficiency with ABTS and dimethyl-4-phenylenediamine, 7 and 32 times better than the wild type, respectively. Computational simulations demonstrated a more favorable binding and electron transfer from the substrate to the T1 copper due to the introduced mutations. PM1 laccase is exceptionally stable to thermal inactivation ($t_{1/2}$ 70 °C = 1.2 h). Yet, both enzymes display outstanding structural robustness at high temperature. They keep folded during 2 h at 100 °C though, thereafter, 7D5 laccase unfolds faster. Rigidification of certain loops due to the mutations added on the protein surface would diminish the capability to absorb temperature fluctuations leading to earlier protein unfolding.

1. Introduction

Laccases (EC 1.10.3.2) are blue-multicopper oxidases capable of oxidizing multiple aromatic compounds such as substituted phenols, aromatic amines, N-heterocycles (indole, benzothiazol, tetrahydroquinoline, hydroxyphthalimide, naphthol, etc), heterocyclic thiols and others, as well as some inorganic/organic metals [1–4]. The paramagnetic blue copper at the T1 site is the responsible of subtracting one electron from the substrate and transferring it to the trinuclear T2/T3 copper cluster, were molecular oxygen is reduced to water [5,6]. Laccases are widespread in nature and can be classified, according to their T1 site as low (<+500 mV, most plant and prokaryotic laccases), medium (+500 to around +700 mV) and high (from +720 to +800 mV) redox potential laccases [7]. The high-redox potential laccases (HRPLs) are only produced by certain fungi such as the white-rot basidiomycetes responsible for lignin decay in nature. In addition to the low requirements of laccases (use of oxygen from the air and release of water as the sole by-product) as compared with peroxidases, HRPLs are of particular interest as biocatalyst for certain oxidation reactions (to replace harsh chemicals and metal catalysts) due to their higher catalytic promiscuity. For instance, they directly oxidize high-redox potential compounds such as aniline, synthetic organic azo-dyes, technical lignins or synthetic redox mediators like 1-hydroxybenzotriazole (HBT) [2,8–11]. The latter has been widely assayed to promote the enzymatic oxidation of recalcitrant compounds [12,13]. With or without mediators, HRPLs can catalyze a huge range of polymerization and degradation oxidative reactions valuable for different industrial sectors such as pulp and paper, textile and food industry, waste decontamination and detoxification and organic synthesis [14].

However, their difficult heterologous expression together with low activity or stability at the required operating conditions is

* Corresponding author.
E-mail address: susanacam@cib.csic.es (S. Camarero).

https://doi.org/10.1016/j.ijbiomac.2019.09.052
0141-8130/

one of the main obstacles for the industrial application of HRPLs, which must be addressed by protein engineering. In recent years, the progress in computational power and the increasing availability of protein crystal structures offered stimulating structure-function knowledge to enzyme engineers. This, combined with the use of directed evolution tools, have notably aid in the design of tailor-made industrial biocatalysts [15]. Enzyme directed evolution allows discovering new hotspots for protein engineering otherwise not revealed by rational strategies, while computational design permits to analyze the mutational space of these hotspots much faster than they can be explored in the lab, thus contributing to reduce the screening effort [16,17]. In previous works, simulation studies helped us to understand the beneficial effect of the mutations accumulated through directed evolution on laccase activity [18,19]. Moreover, they predicted beneficial mutations to enhance laccase activity towards a particular substrate [20], or envisaged the oxidation of a target substrate by different laccases, according to differences in their substrate-binding pockets [21]. These studies mainly consisted of protein-substrate exploration using the Protein Energy Landscape Exploration (PELE) software, in combination with quantum mechanics/molecular mechanics (QM/MM) simulations. In redox systems, such a combination can map the donor-acceptor distance (DAD), the solvent-accessible surface area (SASA) and spin densities of the substrate. In addition, several bioinformatics tools, such as HotSpot Wizard 3.0, RING and CABS-flex 2.0, allow stability predictions associated to position mutability according to evolution conservation, intra-protein contacts and potential protein motions [22,23].

In previous works, two wild HRPLs from basidiomycetes PM1, *Coriolopsis* sp., and *Pycnoporus cinnabarinus*, sharing a 76% of sequence identity, were subjected to parallel directed evolution campaigns for expression in *Saccharomyces cerevisiae* [24,25]. Both laccases were actively secreted by the yeast upon lab evolution of their CDS fused to the prepro leader of the alpha-mating factor of *S. cerevisiae*. In addition, the catalytic activity towards phenolic and non-phenolic compounds was notably increased in the evolved *P. cinnabarinus* laccase, whereas the evolved PM1 laccase recovered the catalytic properties of the wild type. In a further directed evolution step, both evolved enzymes were subjected to DNA shuffling to obtain chimeric laccases functionally secreted by the yeast with combined properties (in terms of optimal pH, substrate affinity or stability) [26]. One of them is 7D5 laccase, which was later used as biocatalyst for the synthesis of conductive polyaniline due to its outstanding capabilities to oxidize aromatic amines [8].

In this work, we fully characterize 7D5 laccase once over expressed in *Aspergillus oryzae* (Novozymes) [8]. Given its higher sequence identity with parent PM1 laccase (as compared to *P. cinnabarinus* laccase), the former was used as the reference wild type enzyme (pdb 5ANH) to evaluate the structural and biochemical modifications observed in the engineered enzyme. Changes in k_{cat} values or enzyme stability were rationalized by computational analyses to assess the contribution of the mutations accumulated in the engineered laccase to the activity and stability of the enzyme.

2. Materials and methods

2.1. Reagents

2,6-dimethoxyphenol (DMP), 2,2′-azino-bis(3-ethylbenzothiazoline-6-sulphonic acid) (ABTS), *N*,*N*-dimethyl-*p*-phenylenediamine (DMPD), aniline, 1-hydroxybenzotriazole (HBT), 4-hydrobenzoic acid (4-HBA), 4-aminoantipyrine (4-AAP) and 2-metoxyphenol (guaiacol) were purchased from Sigma-Aldrich (Madrid, Spain). Endoglycosydase-H (Endo-H) was purchased from Roche (Basel, Switzerland).

2.2. Enzyme production and purification

7D5 laccase was produced in *A. oryzae* [27] at Novozymes, in standard MDU-2BP media containing $CuSO_4$ as described in De Salas et al. 2016 [8]. The enzyme was purified in one step using an anion exchange Mono Q HR 5/5 column attached to a FPLC (AKTA purifier, GE Healthcare) in a 30 mL gradient of 0–25% elution buffer (20 mM Tris-HCl + 1 M NaCl, pH 7). PM1 laccase was produced by PM1 fungus grown in 1 l flasks with 300 ml GAE medium [28] at 30 °C and 180 rpm. After 11 days of incubation, liquid extracts were filtrated (first with filter paper and then using a 0.45-μm cutoff membrane) and concentrated and ultra-diafiltrated using a Pellicon tangential filtration membranes (Merck Millipore, Germany) and Amicon stirred cells (Merck Millipore, Germany), both with a 10 kDa cutoff. PM1 laccase was purified by FPLC in two anion exchange steps: i) HiPrep Q FF 16/10 column in a 100 ml gradient of 0–40% elution buffer; and ii) Mono Q HR 5/5 column in a 30 ml gradient of 0–25% elution buffer. All columns were purchased from GE Healthcare. Fractions containing laccase activity were pooled, dialyzed in Tris-HCl pH 7 and concentrated after each chromatographic step. Enzyme purification was confirmed by the A280/A600 nm ratio of the purified enzymes and their electrophoretic mobility in SDS-PAGE (12% acrylamide) stained with Coomassie brilliant blue.

2.3. Determination of molecular weight and glycosylation degree

Laccases were deglycosylated with Endo-H (0.5 U/5 mg purified laccase, added in two steps) in sodium acetate buffer 50 mM pH 5.5, at 37 °C for 24 h. Enzyme deglycosylation was confirmed by SDS-PAGE electrophoresis (12% acrylamide).

MALDI-TOF-TOF analyses of glycosylated and deglycosylated samples were performed in an Autoflex III instrument (Bruker Daltonics, Bremen, Germany) with a smartbeam laser. The spectra were acquired using a laser power just above the ionization threshold. Samples were analyzed in the positive ion detection and delayed extraction linear mode. Typically, 1000 laser shots were summed into a single mass spectrum. External calibration was performed, using the Protein Standard II from Bruker, covering the range from 15,000 to 70,000 Da. The 2,5-Dihydroxyacetophenone (2,5-DHAP) matrix solution was prepared by dissolving 7.6 mg (50 μmol) in 375 μl ethanol followed by the addition of 125 μl of 80 mM diammonium hydrogen citrate aqueous solution. For sample preparation, 2.0 μl the sample were diluted with 2.0 μl of 2% trifluoroacetic acid aqueous solution and 2.0 μl of matrix solution. A volume of 1.0 μl of this mixture was spotted on the 800 μm AnchorChip target (Bruker-Daltonics) and allowed to dry at room temperature. The molecular weight analysis by MS-MALDI TOF was carried out in Proteomics and Genomics Facility (CIB-CSIC), a member of ProteoRed-ISCIII network.

2.4. X-ray crystallography

X-ray crystallography analysis of 7D5 laccase was carried out after deglycosylation of the enzyme and removal of Endo-H by using a Mono-Q column in a 30 mL gradient of 0–25% elution buffer (20 mM sodium acetate 150 mM NaCl pH 5.7). The enzyme was dialyzed and concentrated in 20 mM Tris-HCl pH 7.

Crystallization trials were set up at 293 K, starting with a condition already published [29]. The best diffracting crystals were obtained by the hanging-drop vapour-diffusion method, in 24-well plates (Hampton Research), after seeding fresh drops consisted on 2 μl of protein at 5 mg ml^{-1} and 1 μl of reservoir solution

(100 mM NaAc, 200 mM Li_2SO_4, 20% (v/v) polyethylenglycol 4000 and 100 mM HEPES pH 7.5). The crystals grew in ~5 days and reached final dimensions of 0.07 × 0.07 × 0.07 mm^3. Prior data collection, they were immersed in the precipitant solution containing 20% (v/v) glycerol, followed by rapid flash cooling in liquid nitrogen. A complete X-ray diffraction data set was collected at the beam line I02 at Diamond Light Source (Harwell Campus, UK). Data were indexed and integrated using XDS [30] and scaled with SCALA from the CCP4 suite [31]. The crystals belonged to the space group I23 with cell dimensions a = b = c = 202.61 Å and α = β = γ = 90°. Matthews coefficient and self-rotation function indicated the presence of two molecules in the asymmetric unit, with a solvent content of 62.23%. Molecular replacement was performed with Phaser [32] using the Protein Data Bank entry 1GYC as model, and the refinement was carried out with PHENIX [33] including rigid body refinement as the first step. Several rounds of iterative refinement and manual building steps were done with Coot [34]. Coordinates and structure factors have been deposited at the PDB with accession code 6H5Y. Model quality was checked using MolProbity implemented within the PHENIX suite. Figures were prepared with Pymol (Molecular Graphics System, Version 1.5.0.4 Schrödinger, LLC). Details of data collection and processing, refinement statistics and quality indicators of the final model are summarized in Table S2.

2.5. Small-angle X-ray scattering

SAXS measurements of laccase in solution were performed at Diamond Light Source beam line B21 (Harwell Campus, UK), using a BioSAXS robot for sample loading, from solutions of the glycosylated and deglycosylated forms of 7D5 laccase at different concentrations in 20 mM Tris-HCl pH 7 at 277 K. Samples of 40 μl corresponding to PM1 laccase glycosylated at 17 mg ml^{-1} and to PM1 deglycosylated at 15 mg ml^{-1}, were delivered via an in-line Agilent 1200 HPLC system in a Shodex Kw-403 column using the same running buffer. During the experiment the samples were exposed for 300 s in 10 s acquisition blocks using a sample to detector distance of 3.9 m and X-ray wavelength of 1 Å. The data were analyzed, buffer-subtracted, scaled, and merged using the Scåtter software package (www.bioisis.net). This software was also used to check possible radiation damage of the samples by visual inspection of the Guinier region as a function of exposure time during data collection. R_G and D_{max} values were calculated with PRIMUS and GNOM, and shape estimation was carried out with DAMMIF/DAMMIN, all these programs included in the ATSAS package [35]. The radius of gyration (R_g) can be obtained from the P(r) function by integrating the function with r^2 over all values of r. The P(r) distribution function is used to describe the paired-set of distances between all of the electrons within the macromolecular structure and is a useful tool for visibly detecting conformational changes within a macromolecule. Real-space scattering profiles of atomic models were calculated using FoxS [36] and the final ab initio models were superimposed with the high-resolution structure using the program SUPCOMB from the ATSAS package. The proteins molecular mass was estimated with SAXSMoW [37]. Figures were prepared with Pymol (Molecular Graphics System, Version 1.5.0.4 Schrödinger, LLC). Details of data collection and processing are summarized in Table S1.

2.6. Determination of redox potential

Laccase redox potential was determined by the poised potential method using the redox couple $Fe(dipyridyl)_2Cl_2/Fe(dipyridyl)_2Cl_3$ in 8 mM MES buffer (pH 5.3). Oxidation of $F(dipyridyl)_2Cl_2$ at each titration point was followed by the decrease in absorbance at 522 nm (ε_{522} = 5974 M^{-1} cm^{-1}) until equilibrium was reached. The concentration of reduced laccase at equilibrium was considered to be 1/4 of the oxidized $Fe(dipyridyl)_2Cl_2$ concentration.

2.7. Optimal pH and stability assays

Laccase pH profiles were determined as shown in Pardo et al 2012 using purified enzymes [26]. pH stability assays were carried out in 2 ml 0.1 mM Britton and Robinson buffer adjusted to pH 2–9, using 0.1 U/ml purified laccase (final activity with 3 mM ABTS pH 3). Then, samples were incubated at 25 °C for 24 h and 20-μl aliquots of each sample were taken at 0, 3, 6 and 24 h and transferred to a 96-well plate to measure the residual activity with 3 mM ABTS pH 3. Relative activities were calculated as a percentage of the initial laccase activity at each experimental pH. All reactions were measured in triplicate. Determination of T_{50}, defined as the temperature at which the enzyme retains 50% of its activity after 10 min of incubation, was carried out as shown in Pardo et al [26]. Laccase half-life values at 50, 60, 70 and 80 °C, thermal inactivation constants and activation energies (E_a) were obtained as shown in Pardo et al [38]. Circular dichroism (CD) analyses by far-UV CD spectroscopy were performed in a spectropolarymeter Jasco J815 associate to Jasco PTC-4235/15 peltier (JASCO Corporation, Japan). The enzyme was diluted to a concentration of 10 μM in buffer Tris-HCl 20 mM pH 7. Denaturalization ramps were set from 50 °C to 95 °C with a slope of 60 °C/h and measured at 220 nm. Besides, 10 μM of the two enzymes were incubated at 100 °C for 24 h, and CD spectra of samples taken at different incubation times were recorded and compared with the CD spectra of the enzymes at room temperature. The CD spectra were collected between 190 and 250 nm with a scanning speed of 10 nm min^{-1}, using a spectral bandwidth of 1 nm and 0.1 cm path length quartz cell (Hellma, Germany). The protein signal was obtained by subtracting buffer spectrum and represented the average of 5 accumulations.

2.8. Kinetic assays

The oxidation of different substrates by purified laccase was carried out in triplicate, in 96-well plates using 0.0013 μM enzyme for DMPD and DMP, 0.0001 μM enzyme for ABTS, 0.013 μM enzyme for guaiacol, 0.13 μM enzyme for HBT and 0.145 μM enzyme for HBA, in 50 mM citrate phosphate buffer pH 3 (for the assay with ABTS), 100 mM sodium acetate buffer pH 5 (for DMP, HBT and guaiacol) or 100 mM sodium acetate buffer pH 4 (for DMPD). Reactions were measured by the increment of absorbance at 418 nm for ABTS (ε_{418} = 36,000 M^{-1} cm^{-1}), 550 nm for DMPD (ε_{550} = 4134 M^{-1} cm^{-1}), 470 nm for DMP (ε_{470} = 27,500 M^{-1} cm^{-1}), 409 nm for HBT (ε_{409} = 321 M^{-1} cm^{-1}) and 470 nm for guaiacol (ε_{470} = 26,600 M^{-1} cm^{-1}) in a plate reader Spectramax Plus (Molecular Devices, CA, USA), in kinetic mode. Kinetic constants for the oxidation of HBA were determined using 4-AAP. For that, increasing equimolar concentrations of 4-HBA and 4-AAP were added to the reaction and the increment of absorbance from the coupling of HBA to 4-AAP (ε_{500} = 12,200 M^{-1} cm^{-1}) was monitored at 500 nm [39]. Initial oxidation rates were plotted against substrate concentration and fitted to a single rectangular hyperbola function using SigmaPlot 10.0 software. Parameter *a* was the k_{cat} and the parameter *b* was equal to the K_m.

2.9. Computational analysis

Protein-ligand interactions were analyzed using HBT and DMPD as substrates with the PELE software. Ligands were optimized in implicit solvent with the density functional M06 and 6-31G* basis

set level of theory using Jaguar from Schrodinger; ESP charges were then extracted for ligand parameterization. The enzymes were prepared with the protein wizard from Schrodinger, at pH 4. PELE is a Monte-Carlo (MC) based software that was developed for mapping protein-ligand interactions, both at the global and local level. Each MC step includes a perturbation and a relaxation phase, before a Metropolis acceptance test accepts or rejects the proposed new pose. Binding energies are then scored using an OPLS-AA protein-ligand interaction energy, which includes a generalized surface born implicit solvent. All simulations involved 100 processors for 48 h, were we applied distance harmonic restraints to all copper's coordination bonds. QM/MM calculations were also performed on 5 randomly-selected structures to estimate the amount of substrate oxidation. This technique partition the system into a classical region (MM) and a quantum one (QM), allowing to describe electronic effects in the frame of the enzyme. The QM region, including the T1 copper, its coordination residues and the substrate, was computed at the DFT (Density Functional Theory) level of theory, with the M06-L functional and the LACVP* basis set. The MM region was treated using the OPLS-2005 force field; residues beyond 10 Å from the catalytic center (T1 copper) were kept frozen. For each selected structure, 5 optimization steps were run, in order to relax the system before the atomic spin densities were extracted. The sum of all atomic spin densities in the substrate depicts the total amount of the unpaired electron (radical) as a result of its oxidation.

Structure stability modeling has also been analyzed by 40-ns MD simulations using CABS-flex, an efficient coarse grained modeling tool for fast simulations of protein structure flexibility [40].

3. Results and discussion

3.1. Physico-chemical and structural characterization

PM1 and 7D5 laccases were purified to homogeneity as confirmed by SDS-PAGE and A280/A600 ratios of 17–19 (Fig. S1A). According to MALDI/TOF-TOF analyses, MW of PM1L is 57,491 whereas it is 57,770–65,000 for 7D5, suggesting a heterogeneous glycosylation of laccase by *A. oryzae*. Glycosylation degrees around 5% for PM1L and 5–17% for 7D5 were found after deglycosylation with Endo-H (Fig. S1B, C).

We explored the glycosylation effect on the structural stability of the enzymes in solution by small-angle X-ray scattering (SAXS), to check how the elimination of the glycans could affect the three-dimensional structure of the protein and interparticle interactions due to the biophysical changes correlated with the bulk of the glycan (Fig. 1). Both enzymes perform as monomeric proteins in solution like the majority of basidiomycete laccases [41], with some exceptions exhibiting homodimeric structures [42,43]. Enzyme deglycosylation decreases the maximum dimension (Dmax) of both monomeric proteins. Nevertheless, N-glycosylation seems to have a special impact on 7D5 laccase where the glycosylated form adopts a geometrical oblate structure that is converted to a somehow spherical form after deglycosylation. By contrast, PM1 L shows a more spherical structure before and after deglycosylation. Clearly, the size of 7D5_deglyco is higher than that found for PML1_deglyco (Fig. 1, Table S1), most probably due to the heavier O-glycosylation of 7D5, in line with what we observed by MALDI/TOF-TOF (Fig. S1C).

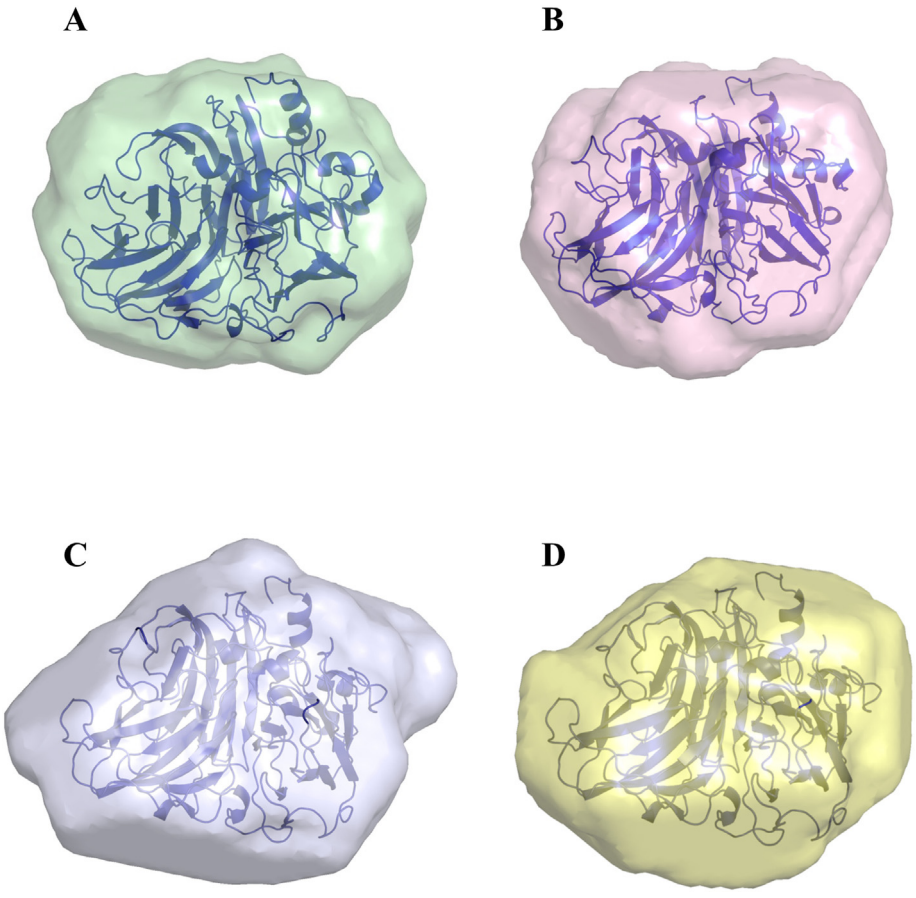

Fig. 1. SAXS structures of glycosylated (A, C) and Endo-H-deglycosylated (B, D) forms of wild type (PM1) laccase (top) and engineered (7D5) laccase expressed in *A. oryzae* (bottom).

To evaluate the influence of the glycan on the intermolecular interactions of 7D5 laccase, SAXS-measurements were done at different concentrations. No indication of strong aggregation was detected during data collection, with data showing linear relationships within the Guinier region (Table S1). The presence of glycans in 7D5 (and PM1 laccase) is easily observed in Fig. S2A-D, which illustrates their corresponding pair distance distribution (P(r)) and clearly shows the presence of additional interatomic distances. This is also reflected in the radius of gyration (Rg) of glycosylated and deglycosylated forms (Table S1). This effect is probably due to a reduction of backbone dynamics due to the presence of the bulky glycans. When comparing the relative shift of heights of the parabola shapes curves in the Kratky plots, it is observed that the deglycosylation forms maintain compact structures similar to the glycosylation forms in both proteins (Fig. S2E-H).

7D5 laccase, derived from the DNA shuffling of evolved PM1L and PcL [26], differs in nine mutations of the wild PM1L (Fig. 2). Mutations V162A, H208Y, S224G, A239P, D281E and S426N accumulated in the protein sequence during the evolution pathway of PM1L for expression in yeast [24], while T291S, E457D and I468T come from the shuffling with evolved PcL parent [25].

The crystal structure of 7D5 laccase (PDB code, 6H5Y) was obtained at 2.3 Å resolution by molecular replacement, using as search model 1GYC. The real space group I23, led us to a solution with two molecules in the asymmetric unit, a Mathews coefficient of 3.26 $Å^3$/Da and a solvent content of ~63%. The structure confirmed the common three-cupredoxin-like-domain folding of fungal laccases [44], quite similar to that of PM1L (PDB code, 5ANH); with a backbone (Ca atoms) rmsd of 0.46 Å and same topology (Fig. 3, table S2). Both crystal structures show equal number of β-strands (30) and α-helixes (7), although mutation I468T enlarges the sixth α-helix in three residues: from VAAT sequence in PM1L, to TPDVAAT sequence in 7D5 (Fig. 2).

Two N-glycosylation sites, Asn54 and Asn433, were found in both molecules, present in the asymmetric unit with well-defined electron densities (Fig. 3). Both sites are highly conserved among basidiomycete laccases, and are considered to play an important role during nascent protein folding, stabilization and secretion [44,45]. However, the higher Dmax and less spherical structure of 7D5 observed by SAXS and the glycosylation percentages deducted from MALDI-TOF/TOF indicate a heavier and more heterogeneous carbohydrate moiety in the enzyme expressed in *A. oryzae*. This fungus possesses two kinds of alpha- 1,2- mannosidases, one located in the ER and the other in the Golgi [46] that would be responsible for highly diverse glycan processing. In addition, and as aforementioned, O-glycosylation seems to be especially important in 7D5 laccase, as suggested by the larger Dmax of the protein after deglycosylation with Endo-H, and in concordance with the formation of branched O-glycans by *Aspergillus* [46].

Up to 72 structures of fungal laccases are deposited in Protein Data Bank, including laccases from Ascomycetes and Basidiomycetes. However, the majority of the 54 basidiomycete laccase structures (from 21 different species) correspond to wild enzymes because of the difficulty to obtain recombinant basidiomycete laccases at high yields [47]. In fact, only two basidiomycete laccases produced heterologously have been crystallized: one from *Coprinus cinereus*, expressed in *A. oryzae* (1HFU and 1A65), and other laccase from *Trametes hirsuta*, expressed in *Penicillium canescens* (5LDU);

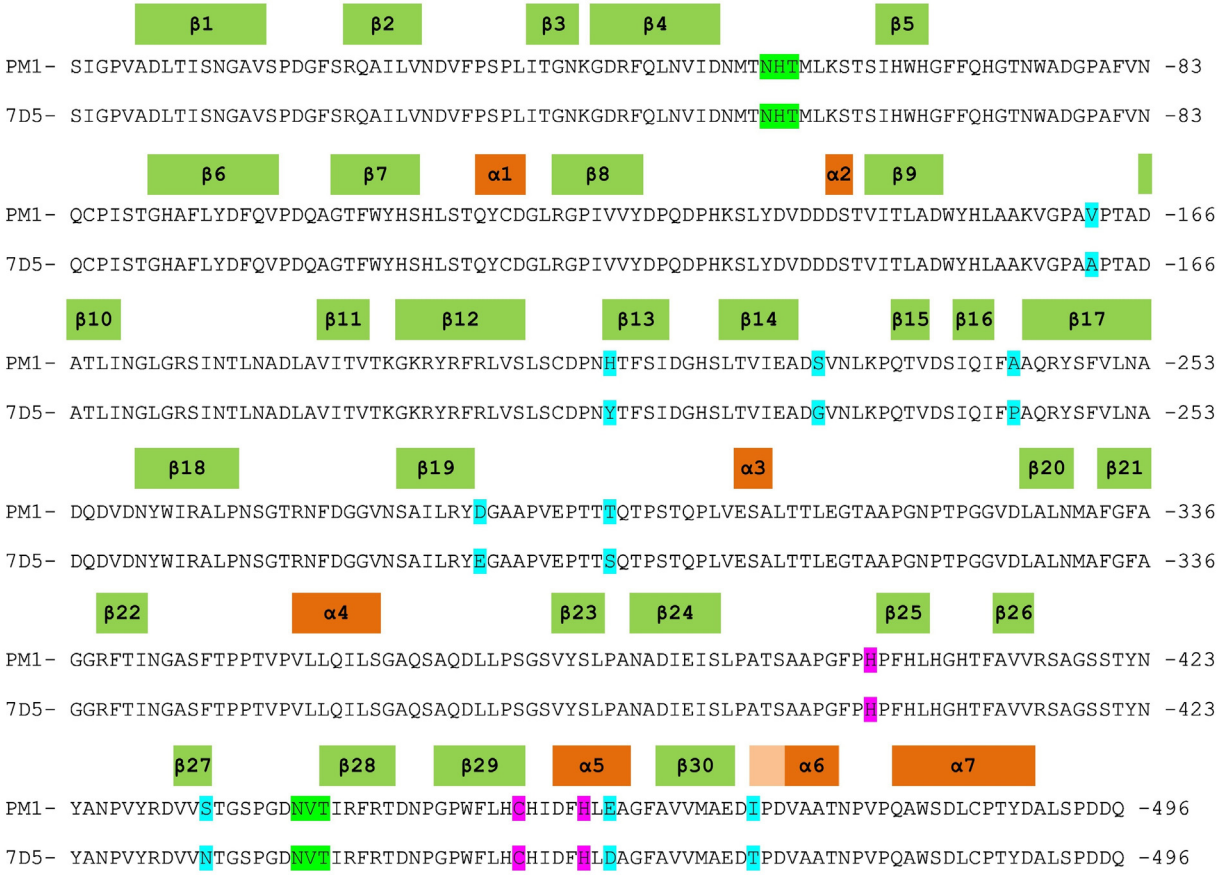

Fig. 2. Comparison of amino acid sequences and numbering of secondary structures in wild PM1 and engineered 7D5 laccases. Location of β-strands are depicted in green and α-helixes in orange (elongation of α-6 in 7D5 laccase due to I468T mutation is shown in light orange). Amino acid replacements between PM1 and 7D5 laccases are shown in cyan, T1-copper coordinating residues in magenta and N-glycosylation sites in bright green. (For interpretation of the references to colour in this figure legend, the reader is referred to the web version of this article.)

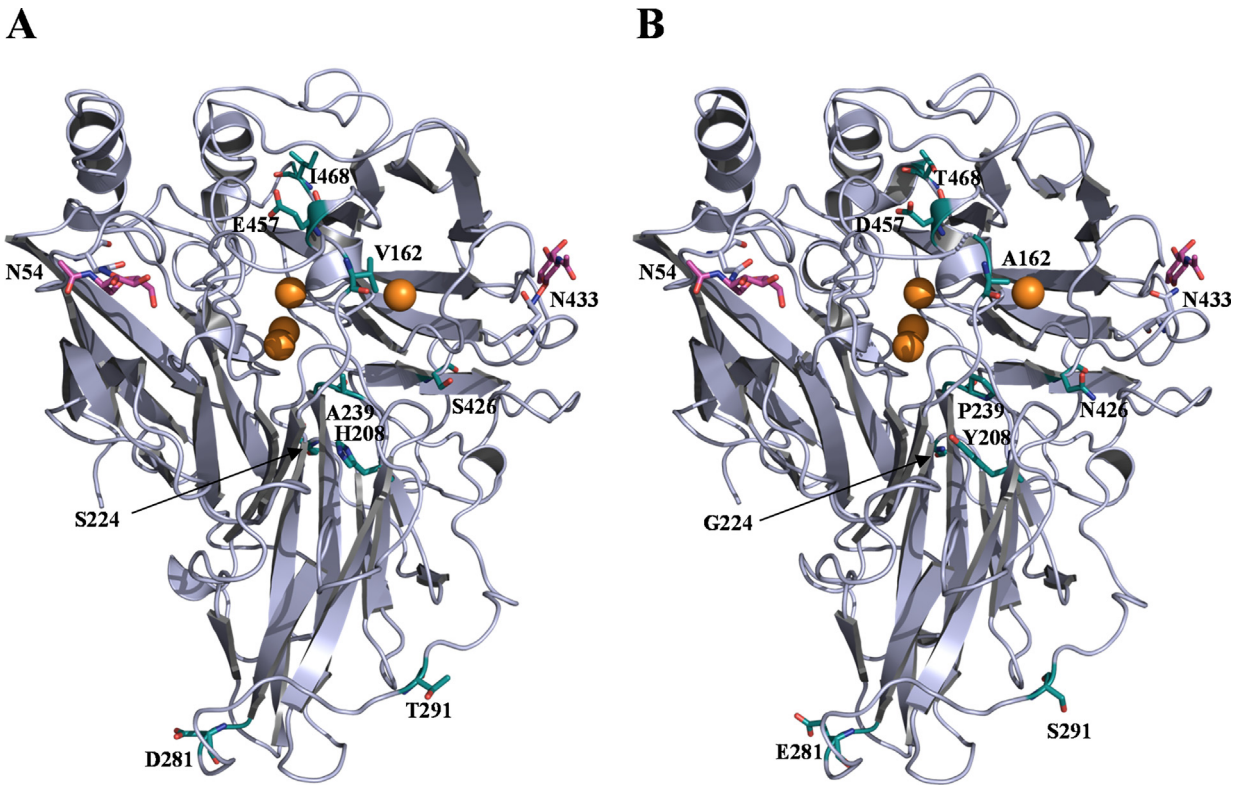

Fig. 3. Cartoon representation for 3D crystal structures of wild PM1 laccase (PDB code 5ANH, A) and engineered 7D5 laccase produced in *A. oryzae* (PDB code 6H5Y, B), showing the catalytic copper ions as orange spheres and the residues mutated during laccase evolution as green-C sticks. N-glycosylation sites (Asn residue) are also depicted as grey-C sticks (with first GlcNAc sugar in magenta-C). (For interpretation of the references to colour in this figure legend, the reader is referred to the web version of this article.)

both of them correspond to native enzymes (Table S3). Conversely, the structural characterization of new variants engineered in the lab might shed light on the protein determinants responsible for modified catalytic activity or robustness, thus providing high-quality information for laccase engineering. Indeed, rational design and enzyme directed evolution techniques are converging in protein science delivering new data for machine learning to accelerate the engineering process [48].

Residues 281, 291 and 468 are located in surface loops far away from the catalytic site, whereas residues 162, 239, 426 and 457 are in the vicinity of the substrate binding pocket (distance to T1 site <10 Å) (Fig. 3). As regards mutations on distal loops of the protein, D281E causes a new H-bond with T190, keeping the interaction with V189 (Fig. 4A, B). In mutation I468T, the introduction of Thr induces a separation from the opposite loop, thus affecting the side-chain conformation of Q359, which rotates to form a salt bridge between its carboxyl oxygen and hydroxyl of T468. Besides, both OE1 and OG1 from Q359, now lie towards the pyrrolidine ring of P469 at a distance of near 3 Å, thus producing a re-structuration of the chain from random coil to alpha helix (Fig. 4C, D). On the other hand, residue 162 is delimiting the substrate binding pocket and residue 457 is in the same α-helix than H455 which coordinates T1 copper. E475 is H-bonded to S113, R335 and D453 in PM1L. Contact with R335 is lost in 7D5 laccase due to E457D mutation and a new H-bond is formed with F454 (Fig. 4E, F).

3.2. Catalytic activity

Substituted phenols 4-hydroxybenzoic acid (HBA), guaiacol and 2,6-dimethoxyphenol (DMP), aromatic amines *N*,*N*-dimethyl-*p*-phenylenediamine (DMPD) and two heterocyclic substrates: 2,2′-azino-bis(3-ethylbenzothiazoline-6-sulphonic acid) (ABTS) and 1-hydroxybenzotriazole HBT) were used to assess laccase's substrate promiscuity. ABTS and DMP are used as standard substrates to assay laccase activity [26]. Besides, ABTS and HBT have been applied as redox mediators, improving the oxidation capabilities of laccase in many biotechnological studies [13,49]. For all the substrates assayed, the evolved 7D5 laccase displayed higher k_{cat} (2–9 fold) values than the wild type (Table 1).

Basidiomycete PM1 is related to *Coriolopsis gallica* and *Trametes trogii* and PM1L is closely related to other HRPLs produced by the above species [28]. When PM1 and 7D5 laccases were compared with these and other *Trametes* laccases, we observed a remarkably superior catalytic activity of 7D5 for ABTS [50]. Although it matches the turnover numbers of *Trametes* laccases at room temperature, its outstanding affinity for this substrate, provides it with a value of catalytic efficiency with ABTS not reported in the literature [50–52]. 7D5 laccase also presents better affinity for DMP although lower k_{cat}. Comparison with other HRPLs like *P. cinnabarinus* laccase confirmed the superior k_{cat} of 7D5 with both substrates [25]. It is worth mentioning that the k_{cat} values obtained here for PM1 and 7D5 laccases with DMP can be underestimated because they were obtained at pH 5 instead at the optimal pH (4).

To sum up, the most remarkable differences in k_{cat} between the wild type and the engineered laccase are obtained for the oxidation of DMP, ABTS and DMPD. The catalytic efficiency was raised 7-fold for ABTS and 3.5-fold for DMP in the engineered enzyme. This would be a consequence of the use of both compounds as substrates for screening the mutant libraries generated during laccase evolution to 7D5 [24,25]. On the other hand, the significant better oxidation of DMPD by 7D5 laccase (with a catalytic efficiency 32 times higher than that of the wild type) was not sought during its design. However, this is not an unexpected result. Due to its superior capability to oxidize aromatic amines, the enzyme had been selected among other counterparts evolved in our lab to carry out the enzymatic synthesis of conducting polyaniline [8] and

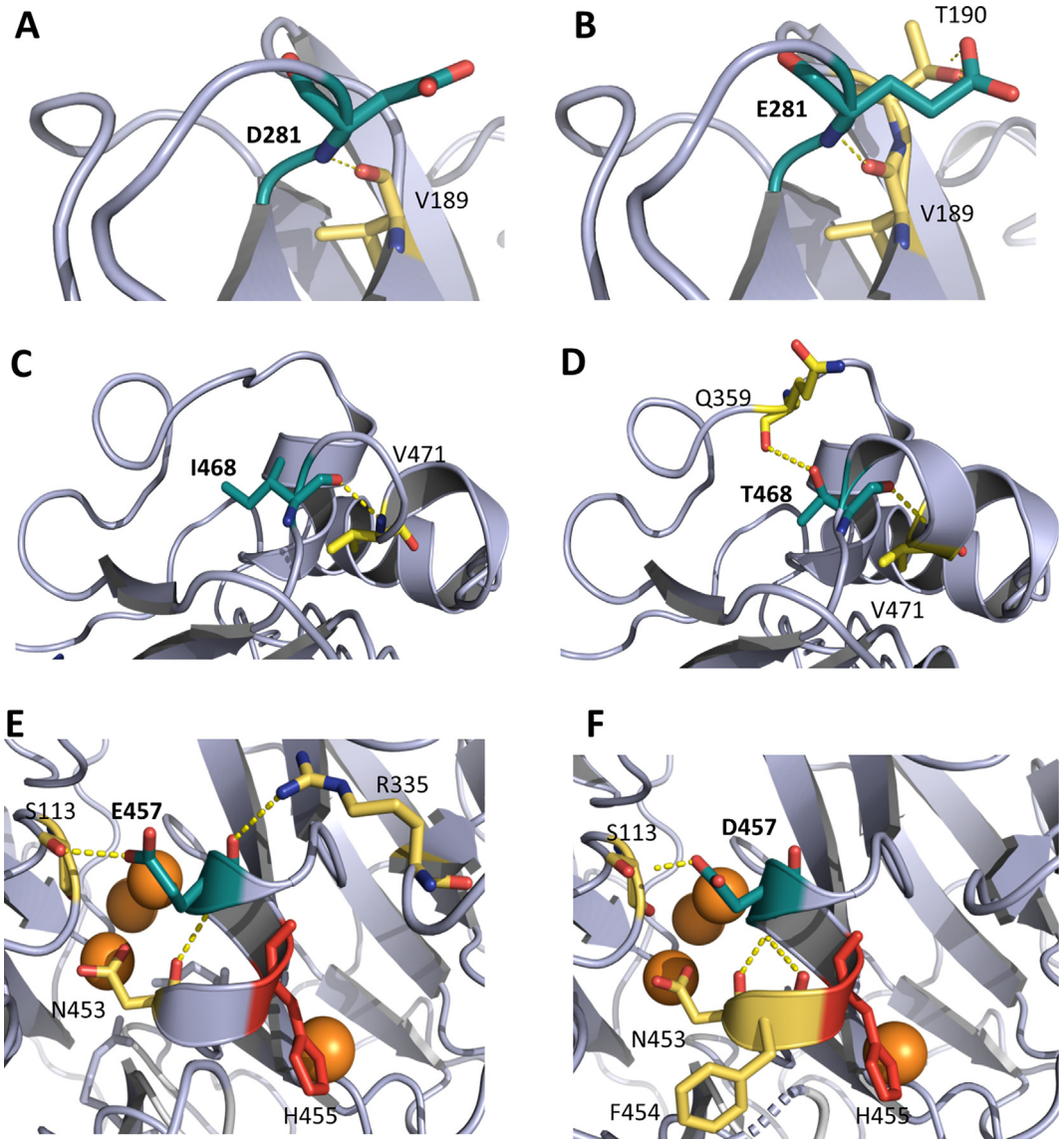

Fig. 4. Close-up of PM1 (left) and 7D5 (right) laccase structures showing the H-bonding of residues 281 (A, B), 468 (C, D), and 457 (E, F).

Table 1
Kinetic constants for the oxidation of different substrates by the engineered (7D5) and wild type (PM1) laccases.

		k_{cat} (s^{-1})	K_m (mM)	k_{cat}/K_m ($mM^{-1}\ s^{-1}$)
ABTS (pH 3)	PM1L	44.4 ± 1.7	0.002 ± 0.0004	26,106 ± 6,222
	7D5L	240.0 ± 11.2	0.0013 ± 0.0002	184,500 ± 29,663
DMP (pH 5)	PM1L	13.2 ± 0.3	0.01 ± 0.001	1325 ± 136
	7D5L	45.3 ± 0.7	0.05 ± 0.003	905 ± 56
Guaiacol (pH 5)	PM1L	2.85 ± 0.05	0.24 ± 0.02	11.9 ± 1.0
	7D5L	10.5 ± 0.2	1.04 ± 0.06	10.1 ± 0.6
HBA (pH 5)	PM1L	3.02 ± 0.12	1.96 ± 0.28	1.54 ± 0.23
	7D5L	8.6 ± 0.2	1.41 ± 0.14	6.1 ± 0.6
DMPD (pH 4)	PM1L	108.6 ± 3.1	1.06 ± 0.06	102 ± 6.5
	7D5L	938.0 ± 29.6	0.29 ± 0.03	3,253 ± 393
HBT (pH 5)	PM1L	15.5 ± 1.0	47.7 ± 6.99	0.33 ± 0.05
	7D5L	28.8 ± 2.4	34.1 ± 6.95	0.84 ± 0.18

thereafter subjected to computational design to improve aniline oxidation at the conditions required for polymerization [20].

The improved catalytic activity of 7D5 is not related to changes in laccase optimal pH or redox potential, given the similar pH profiles and redox potentials of both laccases. The high-redox potential of PM1 laccase ($E^\circ = 0.77 \pm 0.01$ V, referred to NHE standard electrode) was kept in the engineered enzyme ($E^\circ = 0.76 \pm 0.01$ V vs NHE). Both laccases also showed same optimum pH values, pH 2 for ABTS and pH 4 for DMP (Fig. S3) coinciding with the acidic activity profiles characteristic of HRPLs, except for some particular

cases [50,51]. In general, laccases display maximum activities at pH 2–3 for oxidation of ABTS, and slightly less acidic and bell-shaped activity profiles for the oxidation of phenolic compounds due to the counteracting effects: i) decrease in the redox potential of phenol by increasing the pH and ii) inactivation of laccase at alkaline pH because OH^- prevent intramolecular electron transfer [53]. The 20% decrease of activity at pH 2–3 for DMP found in the engineered enzyme would be most probably due to the selective pressure applied during the evolution pathway where mutant libraries were screened with DMP at pH 5 [24,25].

3.3. Simulation analysis

To better study the effect that mutations accumulated in 7D5 laccase have on the improvement of its catalytic activity, PELE simulations were carried out for the wild type and engineered laccase with DMPD and HBT, the substrates with higher and lower k_{cat} increase, respectively. In the case of DMPD, PELE calculations displayed similar binding energies for both enzymes but with a significant decrease of the best catalytic distances in 7D5 (Fig. S4A). For the mediator HBT the binding energy profile shows fewer differences for both enzymes (Fig. S4B). Importantly, 7D5 has a significantly higher number of catalytic events for both substrates, defining them as those structures where the substrate adopts a distance below 4 Å to His455 (the T1 copper ligand responsible for electron subtraction from the substrate) [7]. The increment was more important for DMPD. Comparing the catalytic events populations, we appreciated a large relative increase in 7D5 (418 and 1663 catalytic events for DMPD and HBT) as compared with PM1 laccase (19 and 445, respectively). These results correlate with the kinetic results obtained in the lab and suggest a better positioning of the substrate in the catalytic site. The analysis of these catalytic poses indicates that mutation V162A, one of the hydrophobic residues in the loop that delimits the substrate pocket at the T1 site [54], improves the catalytic poses by opening an additional space in the copper cavity. This would decrease the distance of DMPD substrate to the Cu-H455 moiety (Fig. 5A, B), thus improving the electronic coupling and increasing the electron transfer rate, which correlates with the increase in k_{cat} and decrease in K_m (Table 1). The positive effect of mutation V162A by opening the entrance to the binding cavity was already suggested during the evolution of PM1 laccase [24]. It is worth noting that previous studies carried by our group [18–20] have confirmed the crucial role of catalytic pocket residues in substrate orientation and binding which determine the enzyme activity. Besides due to the crucial location of residue 162, it has been targeted in several focused evolution studies to improve laccase activity by favoring the binding of selected substrates [19,55,56].

We also computed substrates spin density using QM/MM techniques. Spin densities provide the amount of unpaired electrons and thus, they can be used to monitor the extent of electron trans-

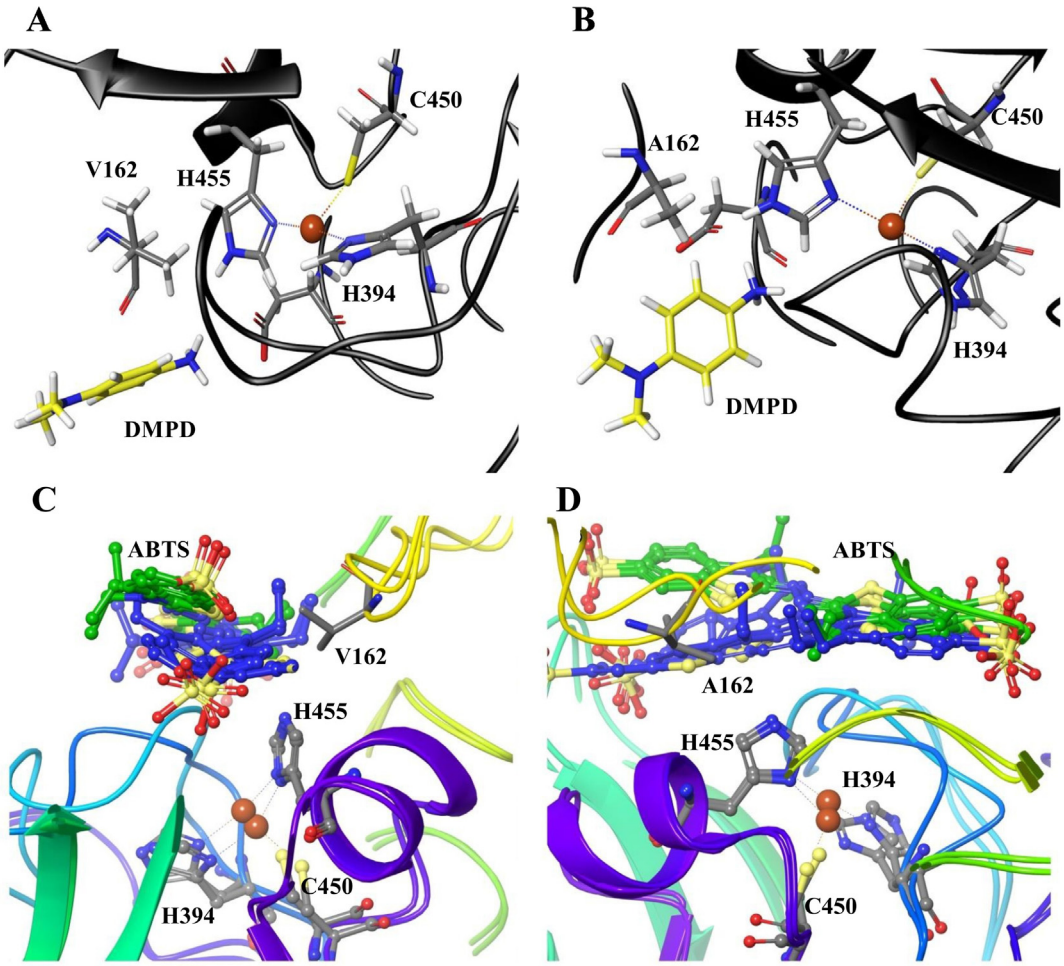

Fig. 5. A representative snapshot of DMPD interaction with the catalytic cavities of PM1 (A) and 7D5 (B) laccases, and two different views (C, D) for ABTS interactions with the binding pocket of PM1 and 7D5 laccases (as green and blue-C colored sticks, respectively). (For interpretation of the references to colour in this figure legend, the reader is referred to the web version of this article.)

fer between the donor and the acceptor, that is, the oxidation. The percentage of spin density in DMPD and HBT for 7D5 is, however, the same as for PM1 laccase (Fig. S4C). This might reflect the fact that, while the substrate gets closer to the catalytic His455 (increase in electronic coupling), its pocket environment remains quite similar (invariance in the substrate oxidation potential). Due to the different nature of ABTS with respect to the other substrates, we performed additional binding and spin density calculations. Interestingly, for this bulkier substrate we find a significant larger conformational change as a result of the reduction in side chain size in the V162A mutation. As seen in Fig. 5C, D, about half of the substrate rearranges its position towards the catalytic His455, considerably reducing its exposure to the solvent and, importantly, increasing its spin density in 7D5 (Fig. S4C) as a result of a local shift in its redox potential.

Previous studies have suggested a change in the substrate oxidation potential due to (mutation induced) rearrangements in the binding site [18]. Our results indicate that this effect might not be important in the smaller substrates, where we observed only a small repositioning (a better approach to the catalytic His) and no significant change in spin densities. In ABTS, however, we observed an almost 20% increase in spin density. Thus, for this mediator, both an increase in the electronic coupling and a local shift in its oxidation potential seem to be responsible for the changes in kinetic parameters.

Qualitatively, we can model if the increase in electronic coupling can derive in a ~8 fold increase in k_{cat} for DMPD. Assuming that such an increase will originate mainly by the change in kET, and using the alternative form of the Marcus equation $kET \approx \exp.[-\beta(r\text{-}r0)]$, we can derive $kET_{7D5} = kET_{PM1L} \exp.(\Delta r)$, assuming the medium constant, β, to be the same in both species and where Δr represents the reduction in the distance the electron must travel. If we take this difference to be between 1.5 Å and 2 Å (based on Fig. S4A) we obtain a change in kET on the 4.5 to 7.4 range, in close agreement with the change observed in k_{cat}. In addition to mutation V162A that opens an additional space in the copper cavity and has a main effect in the outstanding catalytic improvement for oxidizing DMPD, mutation E457D located in the same α-helix than H455, produces a new interaction with contiguous F454. This residue has been described to modulate the enzymatic activity and have also a significant influence on the stability of the enzyme [24,57]. Furthermore, the tripeptide L456-E457-A458 (PM1 laccase numbering) located in this α-helix is highly conserved in HRPLs. The hydrogen bonding between E457 and S113 is characteristic of HRPLs, causing an elongation of the Cu1-N (His455) bond at the T1 site and, therefore raising the E^0 of these laccases [58]. This bond is maintained in 7D5 laccase variant (Fig. 4E,F) due to the conservative nature of mutation E457D, which would explain the preservation of the high-redox potential of the enzyme.

As regards phenolic compounds, we can observe similar behavior of both enzymes for guaiacol and HBA than for DMP. The three molecules have close similar structure and it would be expected that the increase of activity towards DMP obtained for 7D5 during the evolution pathway would be valid for other phenolic compounds. Hence, all the catalytic increment should be associated with a change in the conformation and charge of the catalytic pocket that may favor the substrates oxidation as suggested by the increase of catalytic events and spin densities observed by PELE and QM/MM.

3.4. Enzyme stability

Stabilities of PM1 and 7D5 laccases at pH 2–9 were monitored during 24 h at room temperature. Both were quite stable over pH 6. At pH 6, the wild type maintained its initial activity after 24 h, whereas 7D5 retained 60% of the initial activity. Below pH 6, both enzymes were less stable, although the wild type to a lesser extent. In fact, PM1 laccase displays high stability at extreme pH values. It retains near 100% and 60% of the initial activity after 24 h at pH 9 or pH 2, respectively, whereas 7D5 retained 75% activity at pH 9, but the stability at acidic pH was dramatically diminished (Fig. 6).

On the other hand, the wild type has an outstanding stability to high temperature, displaying a T_{50} (10 min) value of 79 °C (with no decrease of activity until 75 °C), whereas the engineered laccase showed a T_{50} (10 min) value of 65 °C (Fig. 7 A). It is worth mentioning that 7D5 laccase was notably activated at high temperature (laccase activity increased around 60% during the first 5 min of incubation at 75 °C) whereas PM1 laccase was not. The long term kinetic stability proved to be very high for both laccases, with outstanding half-life values for PM1 laccase at 50–80 °C, and with lower but still elevated values for 7D5 (Table 2). For instance, when these data were compared with those from 55 fungal thermotolerant laccases from different basidiomycete and ascomycete strains, only a few showed higher half-lives than PM1 laccase or even its evolved variant, proving the stability of both laccases [59].

The slow thermal inactivation of the wild type was evidenced by its notably low inactivation constants (Table 2). Also, the lower E_a for thermal inactivation of PM1 laccase (175 kJ/mol) than for 7D5 laccase (214 kJ/mol), calculated from Arrhenius the plots (Fig. S5A, B), confirmed the lesser sensitivity to temperature changes of the wild type. Thereafter, we evaluated denaturation of both enzymes by monitoring the changes in typical absorption circular dichroism (CD) bands due to perturbations in secondary

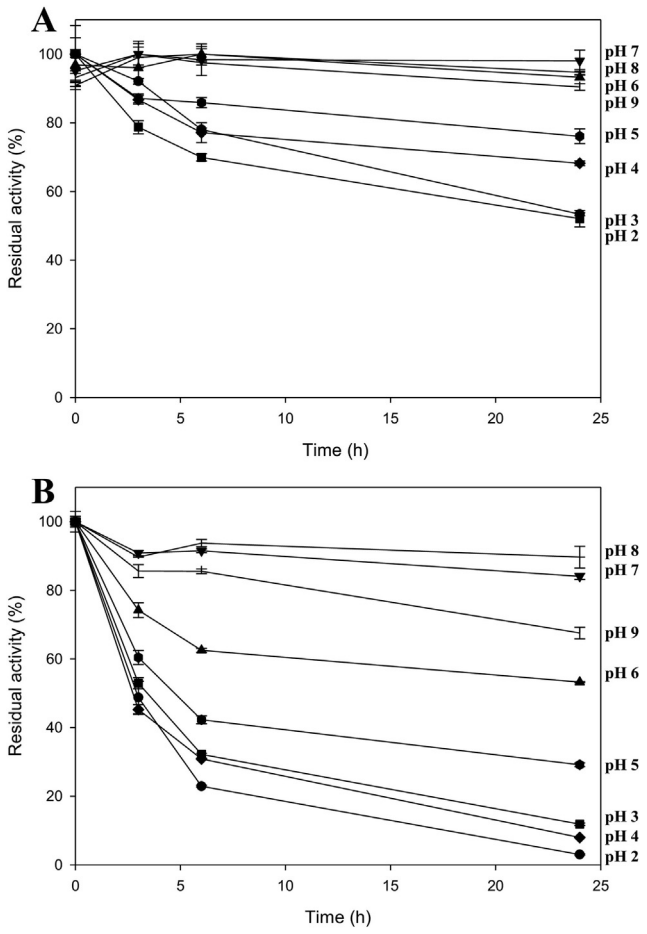

Fig. 6. Stabilities of wild type (PM1) (A) and engineered (7D5) (B) laccases at pH 2–9. Activities at different incubation times were measured with 3 mM ABTS, pH 3.

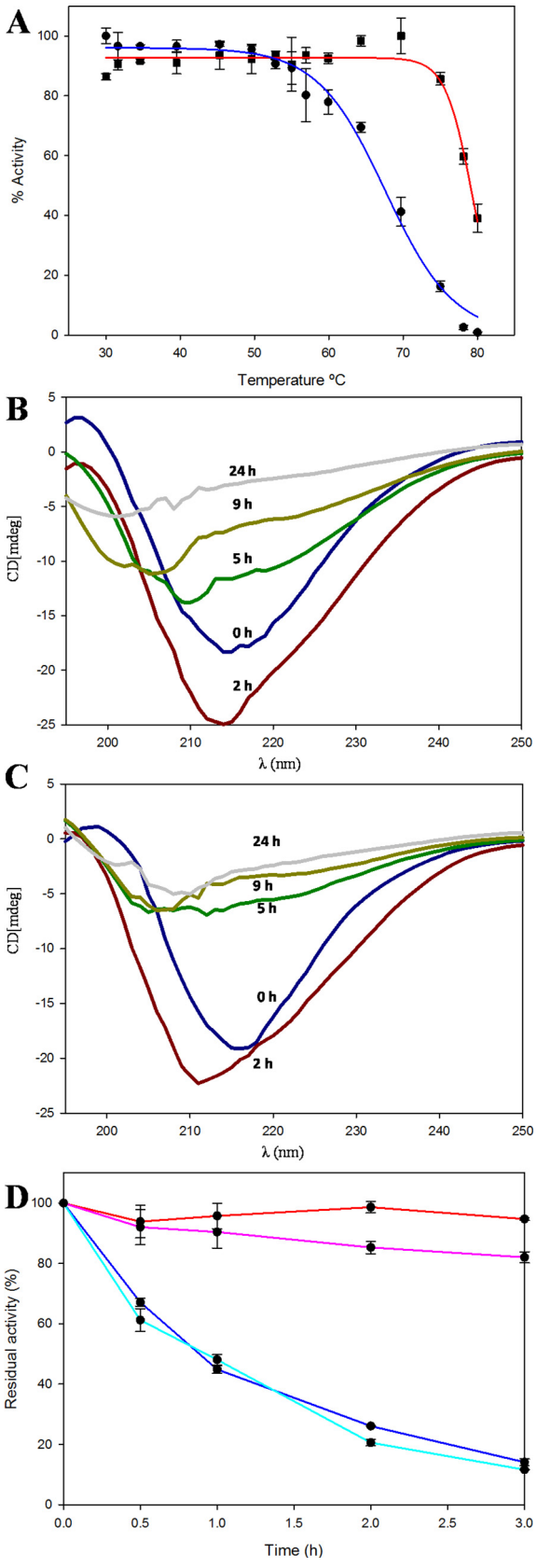

Fig. 7. Comparison of thermal stabilities for PM1 and 7D5 laccases: T50 (10 min) curves for PM1L (red) and 7D5 (blue) (A). CD spectra for thermal denaturation of PM1L (B) and 7D5 (**C**) at 100 °C at different incubation times. Residual activities of PM1L-glyco (red) and PM1L-deglyco (pink) and 7D5_glyco (blue) and 7D5_deglyco (cyan) during incubation at 65 °C (D). (For interpretation of the references to colour in this figure legend, the reader is referred to the web version of this article.)

structures. First, the enzymes were subjected to a temperature ramp between 50 and 95 °C and ellipticity was monitored at 220 nm, the characteristic band for α-helixes (Fig. S5C, D). The intensity of this band didn't decrease and, consequently, no apparent Tm could be calculated for any of the enzymes. In fact, ellipticity values for both enzymes increased once the temperature reached 70 °C. Next, the enzymes were incubated at 100 °C for 24 h and far UV CD spectra were recorded at different incubation times (Fig. 7B,C). Their initial spectra revealed the presence of two dichroic bands: a single negative band with a strong minimum at 216 nm and a positive band with maximum around 196 nm, both typical of antiparallel β-sheet proteins [60]. No protein denaturation was observed during the first 2 h at 100 °C. In fact, even more marked negative band at 216 nm was observed, in particular for PM1 laccase. The initial increments of ellipticity observed in the two CD assays (50–95 °C ramp and 100 °C incubation) suggests the existence of intermediate conformations as a protein adaptation to high temperature. This trend has also been observed in other thermostable laccases, and may be associated to a high structural flexibility at high temperature [38,61–65]. Above 2 h of incubation at 100 °C, the gradual lessening of ellipticity, with the reduction and shift of 216 nm band to lower wavelengths indicative of random-coil polypeptides, and the disappearance of the positive band at 196 nm, evidenced the progress of protein denaturation. Loss of secondary structures was more pronounced and earlier produced in 7D5 laccase, whereas PM1 laccase was not completely unfolded after 5 h of incubation at 100 °C, which is an extremely long incubation time according to data obtained with other stable enzymes [64,66].

To study if the distinct glycosylation of 7D5 and PM1 laccases due to the expression system may influence protein stability, glycosylated and deglycosylated forms of both enzymes were incubated at 65 °C, and residual activities were measured at different incubation times (Fig. 7D). While some differences were found between glycosylated and deglycosylated forms in PM1 laccase, in 7D5, both forms showed close similar thermostability. The main differences were obtained when comparing the wild type and the engineered enzyme, regardless of their glycosylation state (82–94% residual activities for PM1 laccase vs 12–14% for 7D5 variant after 3 h at 65 °C).

The wild type enzyme used in this study comes from a fungal strain (PM1) isolated from the water streams of a paper pulp mill [28] that would explain the outstanding stability to high temperature and alkaline pH of PM1 laccase. Conversely, common activity-stability tradeoff during enzyme evolution would explain the decrement of thermal and pH stability observed in the engineered variant [67–69]. Still, 7D5 laccase maintains high thermostability as compared to other fungal laccases [59], thus confirming DNA-shuffling of homologous genes as an effective strategy to obtain robust enzymes by accumulation of neutral mutations [26,38,70].

Using PyMOL (Delano Scientific LLC) and B-Fitter to calculate the B-factors of laccase structures we can observe a reduction of the flexibility of some of the surface loops were the mutated residues are present. The loop where the mutation D281 is located shows up less flexibility in 7D5 than in PM1 laccase, where more interactions have been found for the mutant variant. Furthermore, loop 356–364 is rigidified by the mutation of the residue I468T that adds and hydrogen bond with residue Q359, as mentioned during the structural analysis of 7D5 (Fig. S4C, D). This interaction also appears in coarse-grained simulations with a high representation frequency (~90% of the simulation). It seems that the reduction of flexibility could affect the enzyme capability to adapt to changes, perturbing the protein thermostability. These results contrast with the traditional assessment of "the higher protein rigidity, the better enzyme thermostability", but they agree with other studies highlighting the fact that rigidity and thermostability

Table 2
Half-lives and thermal inactivation constants of wild type (PM1) and engineered (7D5) laccases at different temperatures.

Temperature	PM1 laccase		7D5 laccase	
	$t_{1/2}$ (h)	k_d (h^{-1})	$t_{1/2}$ (h)	k_d (h^{-1})
50 °C	40.30	0.02	21.70	0.03
60 °C	4.85	0.14	2.80	0.25
70 °C	1.60	0.43	0.22	3.11
80 °C	0.12	5.73	0.03	26.20

are not necessarily correlated [71] or proving the correlation between kinetic stability and thermal flexibility [72]. So far, a variety of alterations in dynamic behavior of thermophilic enzymes, with reductions in certain types of motions and increases in others, have been observed using different techniques [73].

We also performed coarse-grained MD simulations to analyze the overall intra-protein contacts by using CABS-flex. The number of high-frequency contacts (those being formed at least 75% of the simulation length) is closely similar in PM1L and 7D5 (1753 and 1720, respectively). Taking all this into account, the rigidification of certain surface loops in the mutated laccase might affect the thermostability of the enzyme. The CD spectra obtained here for PM1 and 7D5 laccases during first hours at 100 °C seem to corroborate this hypothesis. The ß-sheet folding would be maintained longer in PM1L because the flexible loops would better absorb the impact of high temperatures, keeping longer intact the secondary structures of the backbone. In line with this, two thermostable variants of p-nitrobenzyl esterase generated by directed evolution. Showed mutations conferring more flexibility to surface loops [73]. The gain in thermal stability of mutated hemoglobin has been also correlated with the improved flexibility of a certain loop allowing the protein to concentrate its fluctuations in this single loop and avoid unfolding [74]. Also, a larger flexibility in the CD loop of the globin family has been recently correlated with higher thermostability [71]. Finally, high structural flexibility is characteristic of ancestral proteins which are adapted to high temperature conditions [72].

4. Conclusions

The structure of the laccase solved in this study is, so far, the first crystal structure obtained from a basidiomycete laccase engineered in the lab. Its production at a relevant industrial scale by a hyper-secretory *A. oryzae* strain enabled the deep structural and biochemical characterization of the enzyme. Simultaneously, computational simulations revealed how certain mutations of the catalytic pocket can provide a better positioning of the substrate and improved electronic coupling, thus increasing the electron transfer, or how mutations on the protein surface can affect enzyme stability by reducing the flexibility of the loops. The enzyme studied here holds noteworthy properties such as high-redox potential, overall improved activity and remarkable catalytic efficiency for ABTS and aromatic amines, good stability to high temperature and feasible heterologous overexpression. All together opens new and promising scenarios for its development as an industrial biocatalyst.

Associated content

The Supporting Information includes: Figures, schemes, legends for tables and data sets, materials and methods (PDF).

Accession Codes: The structure factors for the 7D5 crystal structure reported herein have been deposited in the ProteinData Bank as entry 6H5Y.

Group URL: https://www.cib.csic.es/research/microbial-plant-biotechnology/biotechnology-lignocellulosic-biomass.

Author contributions

The manuscript was written by **FS** and **SC** through contributions of all authors. **SC** conceived the work. **FS** produced and purified the enzymes and performed their biochemical and kinetic characterization. **JV** produced 7D5 laccase at Novozymes. **AVG** and **IGM** carried out the crystallization of 7D5 laccase and SAXS analyses. **GS**, **RC** and **VG** are responsible for the computational analyses. **PG** measured redox potentials. **ATM** made a critical review of the manuscript. All authors have given approval to the final version of the manuscript.

Acknowledgements

This work has been funded by the INDOX EU project (KBBE-2013-7-613549), the Spanish projects BIO2017-86559-R and CTQ2016-79138-R, the H2020-iNEXT grant numbers 1676 and ISCIII. This work has received funding from the Bio Based Industries Joint Undertaking (JU) under grant agreement No 792070. The JU receives support from the European Union's Horizon 2020 research and innovation programme and the Bio Based Industries Consortium.

Declaration of competing interest

The authors declare no competing financial interest.

Appendix A. Supplementary data

Supplementary data to this article can be found online at https://doi.org/10.1016/j.ijbiomac.2019.09.052.

References

[1] M. Fabbrini, C. Galli, P. Gentili, Comparing the catalytic efficiency of some mediators of laccase, J. Mol. Catal. - B Enzym. 16 (2002) 231–240, https://doi.org/10.1016/S1381-1177(01)00067-4.
[2] S. Camarero, D. Ibarra, M.J. Martınez, A.T. Martınez, Lignin-derived compounds as efficient laccase mediators of different types of recalcitrant dyes, Appl. Environ. Microbiol. 71 (2005) 1775–1784, https://doi.org/10.1128/AEM.71.4.1775.
[3] S. Saadati, N. Ghorashi, A. Rostami, F. Kobarfard, Laccase-based oxidative catalytic systems for the aerobic aromatization of tetrahydroquinazolines and related N-heterocyclic compounds under mild conditions, European J. Org. Chem. 2018 (2018) 4050–4057, https://doi.org/10.1002/ejoc.201800466.
[4] H.T. Abdel-Mohsen, K. Sudheendran, J. Conrad, U. Beifuss, Synthesis of disulfides by laccase-catalyzed oxidative coupling of heterocyclic thiols, Green Chem. 15 (2013) 1490–1495, https://doi.org/10.1039/c3gc40106e.
[5] E.I. Solomon, U.M. Sundaram, T.E. Machonkin, Multicopper oxidases and Oxygenases, Chem. Rev. 96 (1996) 2563–2606, https://doi.org/10.1080/00032719.2016.1141415.
[6] P. Giardina, V. Faraco, C. Pezzella, A. Piscitelli, S. Vanhulle, G. Sannia, Laccases: a never-ending story, Cell. Mol. Life Sci. 67 (2010) 369–385, https://doi.org/10.1007/s00018-009-0169-1.
[7] I. Pardo, S. Camarero, Laccase engineering by rational and evolutionary design, Cell. Mol. Life Sci. 72 (2015) 897–910, https://doi.org/10.1007/s00018-014-1824-8.

[8] F. De Salas, I. Pardo, H.J. Salavagione, P. Aza, E. Amougi, J. Vind, A.T. Martínez, S. Camarero, Advanced synthesis of conductive polyaniline using laccase as biocatalyst, PLoS One 11 (2016) 1–18, https://doi.org/10.1371/journal.pone.0164958.
[9] H. Claus, G. Faber, H. König, Redox-mediated decolorization of synthetic dyes by fungal laccases, Appl. Microbiol. Biotechnol. 59 (2002) 672–678, https://doi.org/10.1007/s00253-002-1047-z.
[10] H. Hirai, H. Shibata, S. Kawai, T. Nishida, Role of 1-hydroxybenzotriazole in oxidation by laccase from Trametes versicolor. Kinetic analysis of the laccase-1-hydroxybenzotriazole couple, FEMS Microbiol. Lett. 265 (2006) 56–59, https://doi.org/10.1111/j.1574-6968.2006.00474.x.
[11] V. Hämäläinen, T. Grönroos, A. Suonpää, M.W. Heikkilä, B. Romein, P. Ihalainen, S. Malandra, K.R. Birikh, Enzymatic processes to unlock the lignin value, Front. Bioeng. Biotechnol. 6 (2018) 1–10, https://doi.org/10.3389/fbioe.2018.00020.
[12] M.T. Cambria, Z. Minniti, V. Librando, A. Cambria, Degradation of polycyclic aromatic hydrocarbons by rigidoporus lignosus and its laccase in the presence of redox mediators, Appl. Biochem. Biotechnol. 149 (2008) 1–8, https://doi.org/10.1007/s12010-007-8100-4.
[13] S. Camarero, O. García, T. Vidal, J. Colom, J.C. Del Río, A. Gutiérrez, J.M. Gras, R. Monje, M.J. Martínez, Á.T. Martínez, Efficient bleaching of non-wood high-quality paper pulp using laccase-mediator system, Enzym. Microb. Technol. 35 (2004) 113–120, https://doi.org/10.1016/j.enzmictec.2003.10.019.
[14] A.I. Cañas, S. Camarero, Laccases and their natural mediators: biotechnological tools for sustainable eco-friendly processes, Biotechnol. Adv. 28 (2010) 694–705, https://doi.org/10.1016/j.biotechadv.2010.05.002.
[15] F.H. Arnold, The nature of chemical innovation: new enzymes by evolution, Q. Rev. Biophys. 48 (2015) 404–410, https://doi.org/10.1017/s003358351500013x.
[16] E. Monza, S. Acebes, M. Fátima Lucas, V. Guallar, Molecular modeling in enzyme design, toward in silico guided directed evolution, Dir. Enzym. Evol. Adv. Appl. (2017) 257–284, https://doi.org/10.1007/978-3-319-50413-1_10.
[17] J.C. Moore, A. Rodriguez-Granillo, A. Crespo, S. Govindarajan, M. Welch, K. Hiraga, K. Lexa, N. Marshall, M.D. Truppo, "Site and mutation"-specific predictions enable minimal directed evolution libraries, ACS Synth. Biol. 7 (2018) 1730–1741, https://doi.org/10.1021/acssynbio.7b00359.
[18] E. Monza, M.F. Lucas, S. Camarero, L.C. Alejaldre, A.T. Martínez, V. Guallar, Insights into laccase engineering from molecular simulations: toward a binding-focused strategy, J. Phys. Chem. Lett. 6 (2015) 1447–1453, https://doi.org/10.1021/acs.jpclett.5b00225.
[19] I. Pardo, G. Santiago, P. Gentili, F. Lucas, E. Monza, F.J. Medrano, C. Galli, A.T. Martínez, V. Guallar, S. Camarero, Re-designing the substrate binding pocket of laccase for enhanced oxidation of sinapic acid, Catal. Sci. Technol. 6 (2016) 3900–3910, https://doi.org/10.1039/C5CY01725D.
[20] G. Santiago, F. De Salas, M.F. Lucas, E. Monza, S. Acebes, Á.T. Martinez, S. Camarero, V. Guallar, Computer-aided laccase engineering: toward biological oxidation of Arylamines, ACS Catal. 6 (2016) 5415–5423, https://doi.org/10.1021/acscatal.6b01460.
[21] M.F. Lucas, E. Monza, L.J. Jørgensen, H.A. Ernst, K. Piontek, M.J. Bjerrum, Á.T. Martinez, S. Camarero, V. Guallar, Simulating substrate recognition and oxidation in laccases: from description to design, J. Chem. Theory Comput. 13 (2017) 1462–1467, https://doi.org/10.1021/acs.jctc.6b01158.
[22] A. Kuriata, A.M. Gierut, T. Oleniecki, M.P. Ciemny, A. Kolinski, M. Kurcinski, S. Kmiecik, CABS-flex 2.0: a web server for fast simulations of flexibility of protein structures, Nucleic Acids Res. 46 (2018) W338–W343, https://doi.org/10.1093/nar/gky356.
[23] L. Sumbalova, J. Stourac, T. Martinek, D. Bednar, J. Damborsky, HotSpot wizard 3.0: web server for automated design of mutations and smart libraries based on sequence input information, Nucleic Acids Res. 46 (2018) W356–W362, https://doi.org/10.1093/nar/gky417.
[24] D. Maté, C. García-Burgos, E. García-Ruiz, A.O. Ballesteros, S. Camarero, M. Alcalde, Laboratory evolution of high-redox potential laccases, Chem. Biol. 17 (2010) 1030–1041, https://doi.org/10.1016/j.chembiol.2010.07.010.
[25] S. Camarero, I. Pardo, A.I. Cañas, P. Molina, E. Record, A.T. Martínez, M.J. Martínez, M. Alcalde, Engineering platforms for directed evolution of laccase from Pycnoporus cinnabarinus, Appl. Environ. Microbiol. 78 (2012) 1370–1384, https://doi.org/10.1128/AEM.07530-11.
[26] I. Pardo, A.I. Vicente, D.M. Mate, M. Alcalde, S. Camarero, Development of chimeric laccases by directed evolution, Biotechnol. Bioeng. 109 (2012) 2978–2986, https://doi.org/10.1002/bit.24588.
[27] T. Matsui, H. Udagawa, S. Kishishita, D. Skovlund, Q. Jin, Integrating Polynucleotide Library of Interest in Chromosome of Filamentous Fungal Host Cell Using Site-Specific Recombinase Comprises Transforming Filamentous Fungal Host Cell with Nucleic Acid Construct, 2016.
[28] P.M. Coll, J.M. Fernandez-Abalos, J.R. Villanueva, R. Santamaria, P. Perez, Purification and characterization of a phenoloxidase (laccase) from the lignin-degrading basidiomycete PM1 (CECT 2971), Appl. Environ. Microbiol. 59 (1993) 2607–2613. https://aem.asm.org/content/aem/59/8/2607.full.pdf.
[29] V. Sáez-Jiménez, E. Fernández-Fueyo, F.J. Medrano, A. Romero, A.T. Martínez, F. J. Ruiz-Dueñas, Improving the pH-stability of versatile peroxidase by comparative structural analysis with a naturally-stable manganese peroxidase, PLoS One 10 (2015) 1–22, https://doi.org/10.1371/journal.pone.0140984.
[30] W. Kabsch, XDS, Acta Crystallogr. Sect. D Biol. Crystallogr. 66 (2010) 125–132, https://doi.org/10.1107/S0907444909047337.
[31] P. Evans, Scaling and assessment of data quality, Acta Crystallogr. D. Biol. Crystallogr. 62 (2006) 72–82, https://doi.org/10.1107/S0907444905036693.
[32] A.J. McCoy, R.W. Grosse-Kunstleve, P.D. Adams, M.D. Winn, L.C. Storoni, R.J. Read, Phaser crystallographic software, J. Appl. Crystallogr. 40 (2007) 658–674, https://doi.org/10.1107/s0021889807021206.
[33] P.D. Adams, P.V. Afonine, G. Bunkóczi, V.B. Chen, I.W. Davis, N. Echols, J.J. Headd, L.W. Hung, G.J. Kapral, R.W. Grosse-Kunstleve, A.J. McCoy, N.W. Moriarty, R. Oeffner, R.J. Read, D.C. Richardson, J.S. Richardson, T.C. Terwilliger, P.H. Zwart, PHENIX: a comprehensive python-based system for macromolecular structure solution, Acta Crystallogr. Sect. D Biol. Crystallogr. 66 (2010) 213–221, https://doi.org/10.1107/S0907444909052925.
[34] P. Emsley, K. Cowtan, Coot: model-building tools for molecular graphics, Acta Crystallogr. Sect. D Biol. Crystallogr. 60 (2004) 2126–2132, https://doi.org/10.1107/S0907444904019158.
[35] M.V. Petoukhov, D. Franke, A.V. Shkumatov, G. Tria, A.G. Kikhney, M. Gajda, C. Gorba, H.D.T. Mertens, P.V. Konarev, D.I. Svergun, New developments in the ATSAS program package for small-angle scattering data analysis, J. Appl. Crystallogr. 45 (2012) 342–350, https://doi.org/10.1107/s0021889812007662.
[36] D. Schneidman-Duhovny, M. Hammel, J.A. Tainer, A. Sali, FoXS, FoXSDock and MultiFoXS: single-state and multi-state structural modeling of proteins and their complexes based on SAXS profiles, Nucleic Acids Res. 44 (2016) W424–W429, https://doi.org/10.1093/nar/gkw389.
[37] H. Fischer, M. De Oliveira Neto, H.B. Napolitano, I. Polikarpov, A.F. Craievich, Determination of the molecular weight of proteins in solution from a single small-angle X-ray scattering measurement on a relative scale, J. Appl. Crystallogr. 43 (2010) 101–109, https://doi.org/10.1107/S0021889809043076.
[38] I. Pardo, D. Rodríguez-Escribano, P. Aza, F. de Salas, A.T. Martínez, S. Camarero, A highly stable laccase obtained by swapping the second cupredoxin domain, Sci. Rep. 8 (2018) 1–10, https://doi.org/10.1038/s41598-018-34008-3.
[39] M.B. Ettinger, C.C. Ruchhoft, H.J. Lishka, Sensitive 4-Aminoantipyrine method for phenolic compounds, Anal. Chem. 23 (1951) 1783–1788, https://doi.org/10.1021/ac60060a019.
[40] S. Kmiecik, D. Gront, M. Kolinski, L. Wieteska, A.E. Dawid, A. Kolinski, Coarse-grained protein models and their applications, Chem. Rev. 116 (2016) 7898–7936, https://doi.org/10.1021/acs.chemrev.6b00163.
[41] C.M. Rivera-Hoyos, E.D. Morales-Álvarez, R.A. Poutou-Piñales, A.M. Pedroza-Rodríguez, R. RodrÍguez-Vázquez, J.M. Delgado-Boada, Fungal laccases, Fungal Biol. Rev. 27 (2013) 67–82, https://doi.org/10.1016/j.fbr.2013.07.001.
[42] H.X. Wang, T.B. Ng, Purification of a laccase from fruiting bodies of the mushroom Pleurotus eryngii, Appl. Microbiol. Biotechnol. 69 (2006) 521–525, https://doi.org/10.1007/s00253-005-0086-7.
[43] D.S. Yaver, F. Xu, E.J. Golightly, K.M. Brown, S.H. Brown, M.W. Rey, P. Schneider, T. Halkier, K. Mondorf, H. Dalbøge, Purification, characterization, molecular cloning, and expression of two laccase genes from the white rot basidiomycete Trametes villosa, Appl. Environ. Microbiol. 62 (1996) 834–841, https://doi.org/10.1016/j.amjmed.2005.01.060.
[44] M. Orlikowska, M. de J. Rostro-Alanis, A. Bujacz, C. Hernández-Luna, R. Rubio, R. Parra, G. Bujacz, Structural studies of two thermostable laccases from the white-rot fungus Pycnoporus sanguineus, Int. J. Biol. Macromol. 107 (2018) 1629–1640, https://doi.org/10.1016/j.ijbiomac.2017.10.024.
[45] N.J. Christensen, K.P. Kepp, Stability mechanisms of a thermophilic laccase probed by molecular dynamics, PLoS One 8 (2013), https://doi.org/10.1371/journal.pone.0061985.
[46] N. Deshpande, M.R. Wilkins, N. Packer, H. Nevalainen, Protein glycosylation pathways in filamentous fungi, Glycobiology 18 (2008) 626–637, https://doi.org/10.1093/glycob/cwn044.
[47] A. Kunamneni, S. Camarero, C. García-Burgos, F.J. Plou, A. Ballesteros, M. Alcalde, Engineering and applications of fungal laccases for organic synthesis, Microb. Cell Factories 7 (2008) 1–17, https://doi.org/10.1186/1475-2859-7-32.
[48] G. Li, Y. Dong, M.T. Reetz, Can machine learning revolutionize directed evolution of selective enzymes?, Adv Synth. Catal. (2019), https://doi.org/10.1002/adsc.201900149.
[49] U. Moilanen, M. Kellock, A. Várnai, M. Andberg, L. Viikari, Mechanisms of laccase-mediator treatments improving the enzymatic hydrolysis of pre-treated spruce, Biotechnol. Biofuels. 7 (2014) 1–13, https://doi.org/10.1186/s13068-014-0177-8.
[50] G.S. Nyanhongo, G. Gübitz, P. Sukyai, C. Leitner, D. Haltrich, R. Ludwig, Oxidoreductases from Trametes spp. in biotechnology: a wealth of catalytic activity, Food Technol. Biotechnol. 45 (2007) 250–268. http://www.ftb.com.hr/images/pdfarticles/2007/July-September/45-250.pdf.
[51] J. Jordaan, B.I. Pletschke, W.D. Leukes, Purification and partial characterization of a thermostable laccase from an unidentified basidiomycete, Enzym. Microb. Technol. 34 (2004) 635–641, https://doi.org/10.1016/j.enzmictec.2004.02.003.
[52] J. Yan, D. Chen, E. Yang, J. Niu, Y. Chen, I. Chagan, Purification and characterization of a thermotolerant laccase isoform in Trametes trogii strain and its potential in dye decolorization, Int. Biodeterior. Biodegrad. 93 (2014) 186–194, https://doi.org/10.1016/j.ibiod.2014.06.001.
[53] M. Gunne, V.B. Urlacher, Characterization of the alkaline laccase Ssl1 from Streptomyces sviceus with unusual properties discovered by genome mining, PLoS One 7 (2012) 1–8, https://doi.org/10.1371/journal.pone.0052360.
[54] T. Bertrand, C. Jolivalt, P. Briozzo, E. Caminade, N. Joly, C. Madzak, C. Mougin, Crystal structure of a four-copper laccase complexed with an arylamine: insights into substrate recognition and correlation with kinetics, Biochemistry 41 (2002) 7325–7333, https://doi.org/10.1021/bi0201318.

[55] I. Pardo, S. Camarero, Exploring the oxidation of lignin-derived phenols by a library of laccase mutants, Molecules 20 (2015) 15929–15943, https://doi.org/10.3390/molecules200915929.
[56] I. Mateljak, E. Monza, M.F. Lucas, V. Guallar, O. Aleksejeva, R. Ludwig, D. Leech, S. Shleev, M. Alcalde, Increasing redox potential, redox mediator activity, and stability in a fungal laccase by computer-guided mutagenesis and directed evolution, ACS Catal. 9 (2019) 4561–4572, https://doi.org/10.1021/acscatal.9b00531.
[57] D.M. Mate, D. Gonzalez-Perez, M. Falk, R. Kittl, M. Pita, A.L. De Lacey, R. Ludwig, S. Shleev, M. Alcalde, Blood tolerant laccase by directed evolution, Chem. Biol. 20 (2013) 223–231, https://doi.org/10.1016/j.chembiol.2013.01.001.
[58] K. Piontek, M. Antorini, T. Choinowski, Crystal structure of a laccase from the fungus Trametes versicolor at 1.90-Å resolution containing a full complement of coppers, J. Biol. Chem. 277 (2002) 37663–37669, https://doi.org/10.1074/jbc.M204571200.
[59] K. Hildén, T.K. Hakala, T. Lundell, Thermotolerant and thermostable laccases, Biotechnol. Lett. 31 (2009) 1117–1128, https://doi.org/10.1007/s10529-009-9998-0.
[60] N.J. Greenfield, Using circular dichroism spectra to estimate protein secondary structure, Nat. Protoc. 1 (2006) 2876–2890, https://doi.org/10.1038/nprot.2006.202.
[61] M. Mukhopadhyay, R. Banerjee, Purification and biochemical characterization of a newly produced yellow laccase from Lentinus squarrosulus MR13, 3 Biotech 5 (2015) 227–236, https://doi.org/10.1007/s13205-014-0219-8.
[62] B.A. Kikani, S.P. Singh, Enzyme stability, thermodynamics and secondary structures of α-amylase as probed by the CD spectroscopy, Int. J. Biol. Macromol. 81 (2015) 450–460, https://doi.org/10.1016/j.ijbiomac.2015.08.032.
[63] R.P. Bonomo, G. Cennamo, R. Purrello, A.M. Santoro, R. Zappalà, Comparison of three fungal laccases from Rigidoporus lignosus and Pleurotus ostreatus: correlation between conformation changes and catalytic activity, J. Inorg. Biochem. 83 (2001) 67–75, https://doi.org/10.1016/S0162-0134(00)00130-6.
[64] V. Ferrario, A. Chernykh, F. Fiorindo, M. Kolomytseva, L. Sinigoi, N. Myasoedova, D. Fattor, C. Ebert, L. Golovleva, L. Gardossi, Investigating the role of conformational effects on laccase stability and hyperactivation under stress conditions, ChemBioChem 16 (2015) 2365–2372, https://doi.org/10.1002/cbic.201500339.
[65] A. Karshikoff, L. Nilsson, R. Ladenstein, Rigidity versus flexibility: the dilemma of understanding protein thermal stability, FEBS J. 282 (2015) 3899–3917, https://doi.org/10.1111/febs.13343.
[66] D.W. Sammond, N. Kastelowitz, B.S. Donohoe, M. Alahuhta, V.V. Lunin, D. Chung, N.S. Sarai, H. Yin, A. Mittal, M.E. Himmel, A.M. Guss, Y.J. Bomble, An iterative computational design approach to increase the thermal endurance of a mesophilic enzyme, Biotechnol. Biofuels. 11 (2018) 1–13, https://doi.org/10.1186/s13068-018-1178-9.
[67] N. Tokuriki, D.S. Tawfik, Stability effects of mutations and protein evolvability, Curr. Opin. Struct. Biol. 19 (2009) 596–604, https://doi.org/10.1016/j.sbi.2009.08.003.
[68] P.A. Romero, F.H. Arnold, Exploring protein fitness landscapes by directed evolution, Nat. Rev. Mol. Cell Biol. 10 (2009) 866–876, https://doi.org/10.1038/nrm2805.
[69] R. Kurahashi, S. Sano, K. Takano, Protein evolution is potentially governed by protein stability: directed evolution of an esterase from the hyperthermophilic archaeon Sulfolobus tokodaii, J. Mol. Evol. 86 (2018) 283–292, https://doi.org/10.1007/s00239-018-9843-y.
[70] J.D. Bloom, Z. Lu, D. Chen, A. Raval, O.S. Venturelli, F.H. Arnold, Evolution favors protein mutational robustness in sufficiently large populations, BMC Biol. 5 (2007), https://doi.org/10.1186/1741-7007-5-29.
[71] L. Julió Plana, A.D. Nadra, D.A. Estrin, F.J. Luque, L. Capece, Thermal stability of globins: implications of flexibility and heme coordination studied by molecular dynamics simulations, J. Chem. Inf. Model. 59 (2019) 441–452, https://doi.org/10.1021/acs.jcim.8b00840.
[72] V.A. Risso, S. Martinez-rodriguez, A.M. Candel, D.M. Kru, D. Pantoja-uceda, F. Santoyo-gonzalez, E.A. Gaucher, S.C.L. Kamerlin, M. Bruix, De novo active sites for resurrected Precambrian enzymes, Nat. Comun. 8 (2017) 1–13, https://doi.org/10.1038/ncomms16113.
[73] P.L. Wintrode, D. Zhang, N. Vaidehi, F.H. Arnold, W.A.G. Iii, Protein dynamics in a family of laboratory evolved thermophilic enzymes 2836 (2003) 745–757, https://doi.org/10.1016/S0022-2836(03)00147-5.
[74] J.P. Bustamante, A. Bonamore, A.D. Nadra, N. Sciamanna, A. Bof, D.A. Estrin, L. Boechi, Molecular basis of thermal stability in truncated (2/2) hemoglobins, Biochim. Biophys. Acta 1840 (2014) 2281–2288, https://doi.org/10.1016/j.bbagen.2014.03.018.